NCC3-1022

A Materials Compatibility and Thermal Stability Analysis of Common Hydrocarbon Fuels

M. L. Meyer
NASA Glenn Research Center
Cleveland, Ohio

B. R. Stiegemeier
University of Toledo
Toledo, Ohio

ABSTRACT

A materials compatibility and thermal stability investigation was conducted using five common liquid hydrocarbon fuels and two structural materials. The tests were performed at the NASA Glenn Research Center Heated Tube Facility under environmental conditions similar to those encountered in regeneratively cooled rocket engines. Scanning-electron microscopic analysis in conjunction with energy dispersive spectroscopy (EDS) was utilized to characterize the condition of the tube inner wall surface and any carbon deposition or corrosion that was formed during selected runs. Results show that the carbon deposition process in stainless steel tubes was relatively insensitive to fuel type or test condition. The deposition rates were comparable for all fuels and none of the stainless steel test pieces showed any signs of corrosion. For tests conducted with copper tubing, the sulfur content of the fuel had a significant impact on both the condition of the tube wall and carbon deposition rates. Carbon deposition rates for the lowest sulfur fuels (2 ppm) were slightly higher than those recorded in the stainless steel tubes with no corrosion observed on the inner wall surface. For slightly higher sulfur content (25 ppm) fuels, nodules that intruded into the flow area were observed to form on the inner wall surface. These nodules induced moderate tube pressure drop increases. The highest sulfur content fuels (400 ppm) produced extensive wall pitting and dendritic copper sulfide growth that was continuous along the entire tube wall surface. The result of this tube degradation was the inability to maintain flow rate due to rapidly increasing test section pressure drops. Accompanying this corrosion were carbon deposition rates an order of magnitude greater than those observed in comparable stainless steel tests. The results of this investigation indicate that trace impurities in fuels (i.e. sulfur) can significantly impact the carbon deposition process and produce unacceptable corrosion levels in copper based structural materials.

INTRODUCTION

NASA and the United States Air Force have had extensive interest in advanced propulsion systems (rocket, air-breathing, and combined cycle systems) operated with hydrocarbon fuels. In many cases these propulsion systems are intended to be reusable, low cost, and safe to operate. As these propulsion devices evolve and designers look for ways to improve engine performance, primarily through increasing operating pressures, the strain placed on fuels used to cool engine components simultaneously increases. In some cases, the heat load, which is almost directly proportional to increases in operating pressure, may more than double. With the flow rate of fuel available for cooling purposes limited, the only way to absorb this increase in heat load is to increase the temperature at which the fuel must operate. Additionally, to transfer the energy from the combustor to the coolant, it is desirable to have combustor walls operating at temperatures as high as possible.

Unfortunately, experience has shown that hydrocarbon fuels, at sufficiently high temperatures, begin to decompose resulting in the formation of gums and solids that can deposit on wetted fuel surfaces. The deposit then acts as an insulating layer, causing a further increase in wall temperature, which can eventually lead to loss of structural integrity and propulsion system failure. Excessive deposits may also reduce the coolant flow area and increase surface roughness, resulting in increased coolant pressure drop or reduced coolant flow rate. The rate at which the deposition process occurs is driven by many factors such as wall temperature, fuel composition (e.g. sulfur and oxygen content), velocity (residence time), and coolant passage material. At the present time, the interaction of these effects is not completely understood and the prediction of deposition remains difficult. However, it is generally accepted that at lower temperatures, less than about 900 °F, the deposition process occurs as the result of auto-oxidation reactions, whereas the deposition process at higher temperatures is driven by the pyrolysis of the hydrocarbon molecules.[1] An additional complication has been reported when fuel-bound sulfur is present in fuels used to cool copper and copper alloys structures. The sulfur reacts with the copper to form copper sulfides. This sulfide corrosion can both damage the copper surface and disturb the flow.

This study is part of a larger effort coordinated between NASA and the US Air Force to understand the feasibility of applying a variety of fuels with different characteristics to the various propulsion systems being investigated by the respective organizations. Thus, a series of tasks have been initiated to study both combustion and cooling performance of several readily available aerospace fuels. The purpose of the effort discussed here was to experimentally investigate, using resistively heated tube sections, the heat transfer, thermal stability, and compatibility (with stainless steel and copper) characteristics of five common hydrocarbon fuels: JP-7, JP-8, JP-8+100, JP-10, and RP-1. The experiments were conducted under conditions similar to those encountered in current expendable, regeneratively cooled, hydrocarbon rocket engines.[2, 3] The fuels were chosen as representing most of the fuels used today for aerospace vehicle propulsion: JP-7 is the Air Force's highest thermal stability fuel, used in the SR-71; JP-8 is the standard kerosene fuel for the United States Air Force and Army; JP-8+100 is JP-8 with an additive package that has been shown to markedly improve thermal stability; JP-10 is a higher density hydrocarbon fuel used in cruise missiles and a candidate for several trans–atmospheric vehicles (also the only pure component fuel tested, exotetrahydrodicyclopentadiene); and RP-1 is the long accepted standard propellant for U.S. hydrocarbon rocket engines.

An earlier report presented the results of carbon deposition measurements from these experiments.[4] Recently, a number of remaining pieces of the test articles from those experiments were sectioned and examined with Scanning Electron Microscopy (SEM), and the interior surfaces were analyzed for elemental composition. The results of that effort provide additional insight into the mechanisms involved in the degradation of cooling capability and deposit formation and are presented in this report.

BACKGROUND

Scanning electron microscopy (SEM) and associated compositional analytical techniques have been used in previous efforts to characterize the deposits formed in both laboratory and fielded components. In the gas turbine field, Schirmer published an extensive set of micrographs of the deposits found in an assortment of rigs and engine fuel components.[5] The deposits were primarily carbon compounds, which had condensed from the fuel in the form of spherical particles and collected on the fuel system surfaces. Schirmer characterized these particles as soft and subject to fusion on the heated surface. And noted that under certain conditions, they could be transformed into different forms of deposits: smoother, denser varnishes, for example. In references 6 - 8, which were more similar to the present experiments in operating conditions, dendritic structures were also observed protruding from copper or copper alloy surfaces. Analysis indicated that these dendrites were composed largely of copper and were also referred to as "copper wool." In experiments reported in reference 8, the possibility that the dendritic structures were caused by reaction of the fuel-bound sulfur with the copper in the test section surface was investigated by doping fuels (RP-1, methane, propane) with additional sulfur compounds (thianaphthene, benzyl disulfide), and indeed an increase in the dendritic formations was observed after increasing the fuel sulfur content. In addition, the dendrite formations were identified as copper sulfides.

The carbon deposits formed in sections of each test piece discussed in this paper were previously quantified with a burn-off technique and reported in reference 4. One of the key results reported was a dramatic difference between the tests in SS 304 and Copper 101 test pieces. While the results in SS 304 tubes showed little fuel-to-fuel difference in the rate of deposit formation, in Copper 101 the JP-8 and JP-8+100 had much higher deposit rates than the other fuels (figure 1). Furthermore, the Copper 101 and JP-8 and JP-8+100 tests were terminated after only a few minutes due to significant increases in pressure drop required to maintain coolant flow rate. In reference 4 it was suggested that the increase in deposits was due to the significantly higher sulfur content in the JP-8 and JP-8+100 fuels.

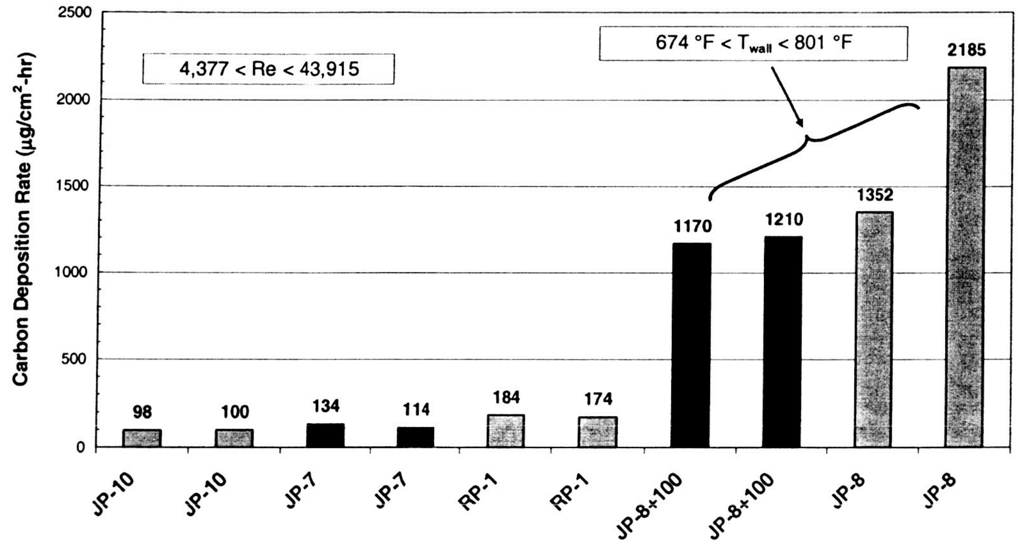

Figure 1: Carbon deposition rates for copper tubes (Tw = 1000 °F; V = 25 ft/s).

EXPERIMENT

A series of heated tube tests was conducted at the NASA Glenn Research Center Heated Tube Facility (HTF) in Cleveland, Ohio using the combustible liquid flow system. A detailed discussion of the experimental design, the facility and the test hardware was presented in reference 4. A brief summary of the experiment is provided here for clarity.

DESIGN OF EXPERIMENT

The primary variables investigated in these experiments were fuel type (five types), wetted wall material (two types), flow velocity (two levels), and inside wall temperature (two levels). Coolant bulk outlet temperature and pressure were held constant. In order to further reduce the number of tests and increase the statistical significance of the results, a half-factorial test matrix was selected with several conditions repeated. The tests conducted for each fuel are defined in table 1. One disadvantage of the half-factorial test matrix selected is that a direct test-to-test comparison of the variation of a single parameter, other than fuel type, is not possible. The two conditions shaded in table 1 were the focus of the present work, as they were the most severe conditions tested for each tube wall material.

Table 1: Test Matrix Summary for Each Fuel

Material	Inner Wall Temp. (°F)	Average Velocity (FT/SEC)
SS 304	750	25
SS 304†	1000	75
Copper 101	750	75
Copper 101†	1000	25
Bulk Outlet Temperature 500°F	Average Pressure 1000 psi	†Repeat Condition

The wall temperatures and coolant flow velocities in table 1 were selected as representative of current expendable RP-1 fueled engines.[2, 3] Coolant outlet temperatures for all tests were set to 500 °F, while mean test section pressures were fixed at 1000 psi. The outlet temperature was chosen to be sufficiently below (≈ 250 °F) the critical temperature of the fuels to avoid the dramatic thermophysical property changes of the bulk flow that would result from operating near reduced temperatures (T/T_c) of one. Run times for all tests were nominally set to twenty minutes. This was predicted to be long enough to produce sufficient coke for analysis, but would still keep fuel quantity requirements low. In some cases test were stopped short due to increasing coolant pressure drop.

FACILITY AND HARDWARE

A simplified schematic of the facility architecture is shown in figure 2.[4] Ambient temperature fuel is loaded into the run tank and pressurized up to 1500 psig. Flow rate and test section pressure are regulated by two valves. Two independent closed-loop controllers operate these valves based on flow rate measurement and test section backpressure measurement to maintain the desired test section flow and pressure conditions.

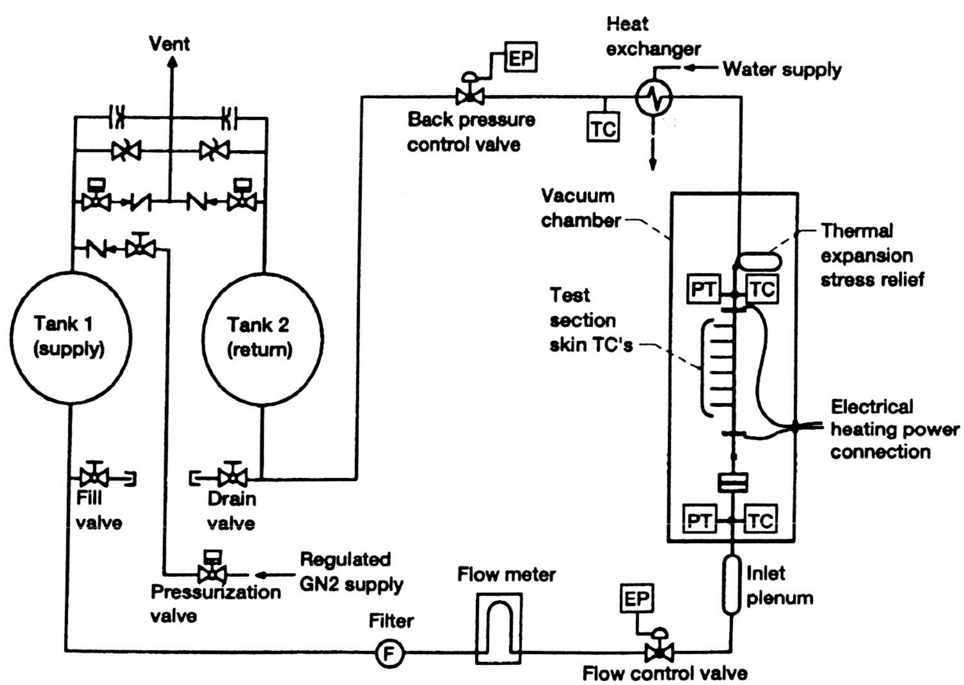

Figure 2. Simplified schematic of the NASA Glenn Heated Tube Facility.

The test sections for these tests were fabricated from drawn tubing of oxygen free electrical copper (Copper 101) and 304 stainless steel (SS 304). The test section dimensions are shown in tables 3 and 4, and they were typically instrumented with four or five outer wall thermocouples, which were spot welded to the SS 304 test sections and brazed to the copper test sections. The properties of JP-10 were sufficiently different from the other fuels to require a change in the test section dimensions to meet the test matrix conditions.

Table 3: Dimensions and Relevant Operating Conditions for JP-7, JP-8, JP-8+100, and RP-1 Test Pieces

Material	**Velocity** (ft/sec)	**Wall Temp.** (°F)	**Inside Dia.** (in)	**Heated Length** (in)	**Heat Flux** (BTU/in^2-sec)	**Flow Rate** (lb_m/sec)
SS 304	25	750	0.06175	14.40	2.20	0.024
SS 304	75	1000	0.06175	11.70	8.10	0.072
Copper 101	25	1000	0.061	8.10	3.90	0.024
Copper 101	75	750	0.061	16.75	5.60	0.070

Table 4: Dimensions and Relevant Operating Conditions for JP-10 Test Pieces

Material	**Velocity** (ft/sec)	**Wall Temp.** (°F)	**Inside Dia.** (in)	**Heated Length** (in)	**Heat Flux** (BTU/ in^2-sec)	**Flow Rate** (lb_m/sec)
SS 304	25	750	0.06175	13.50	2.00	0.027
SS 304	75	1000	0.06175	10.00	8.10	0.081
Copper 101	25	1000	0.061	7.60	3.60	0.027
Copper 101	75	750	0.061	15.50	5.20	0.080

FUEL ANALYSIS

Each of the fuels tested in this study was delivered with a vendor test report verifying that they met the requirements of the respective military specification. Since sulfur has been identified as an important contaminant in previous work with copper, it was necessary to have accurate characterization of the sulfur contamination. In general, the standard sulfur analyses required by the specifications were not sufficiently accurate for the low sulfur fuels. Thus, additional analyses for total fuel-bound sulfur present (e.g. disulfides, mecaptans, thiophenes) were conducted according to standard ASTM test methods. The lower sulfur content fuels were analyzed using the ASTM D 5453, while the ASTM D 4294 was performed on JP-8 and JP-8+100. The

Table 5: Fuel Total Sulfur Content

Fuel	**Total Sulfur Content (ppm)**
JP-7	2 †
JP-8 and JP-8+100	400 *
RP-1	23 †
JP-10	Not Analyzed
† ASTM D 5453	* ASTM D 4294

reproducibility of the test methods is dependant upon the amount of sulfur in the sample, but for the ranges seen in these tests the reproducibility is approximately 2 ppm for the ASTM D 5453 and 100 ppm for the ASTM D 4294. The results of the total sulfur content tests are shown below in table 5. It has been reported previously that certain fuel-bound sulfur compounds are more reactive than others, however, results of speciation of the sulfur compounds in the test fuels is not available at this time.

MICROSCOPIC ANALYTICAL TECHNIQUES

Segments of each test section were milled to expose the interior surface for examination under a scanning electron microscope (SEM) as shown in the sketch in figure 3. In conjunction with the SEM imaging, energy dispersive spectroscopy (EDS) was utilized to perform elemental composition analysis on the inner wall of the tube samples. The EDS technique works by measuring the number and energy of X-rays emitted by the sample after being irradiated by an electron beam. By matching the energy of the emitted X-rays to the known characteristics of each element, the composition of the sample can be determined. It is important to recognize that the highly irregular surfaces analyzed in this investigation are not optimal for EDS analysis and that corrections for the atomic number, absorption, and possible fluorescence of the elements are all possible sources of errors in the quantification process. Even with these limitations, the qualitative information provided by the EDS analysis provides significant insight into the deposition and corrosion processes. All of the results given below were obtained using a standardless calibration at an accelerating voltage of 10kV.

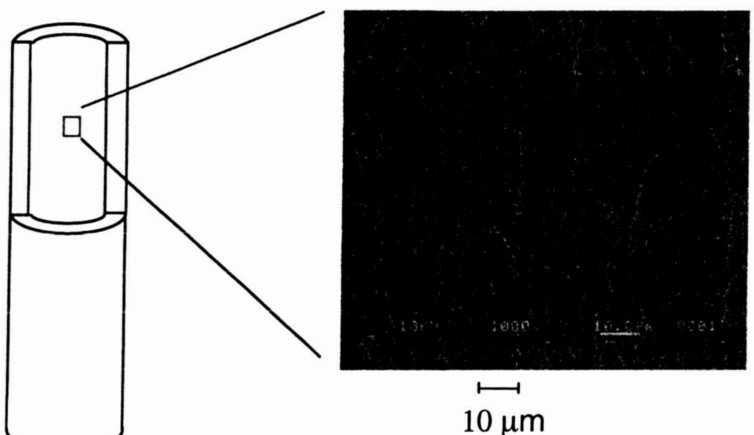

Figure 3. SEM micrograph of a clean section of Copper 101 tubing showing the as delivered internal surface due to the drawing process.

RESULTS AND DISCUSSION

A series of micrographs are presented in figures 4-8 and illustrate the most significant results of the microscopic imaging effort. In figure 4, four images magnified 1000x are presented from approximately the same location in four different test sections, which were operated with each of the fuels at approximately the same test conditions. The one exception was that the JP-8 test was only 2 minutes in duration compared with 20 minutes for the other fuels (note that JP-8 and JP-8+100 were similar and so separate results are not presented). The four fuels show a significant range in corrosion/deposition behavior. It is also apparent that the sulfur content of the fuel is a significant contributor to the corrosion/deposition process.

JP-8, with the highest sulfur content (400 ppm), in just two minutes formed dendritic structures that dominate the corrosion/deposition process and nearly fill the test section. The flow passage was not completely plugged in this test, but coolant pressure drop more than doubled, forcing early termination of the test. At approximately 23 ppm sulfur content, RP-1 formed some nodules (lighter colored structures) and darker deposits on the surfaces between the nodules. JP-7, a very low sulfur fuel at 2 ppm total sulfur, did not form any nodules in the 20 minute test.

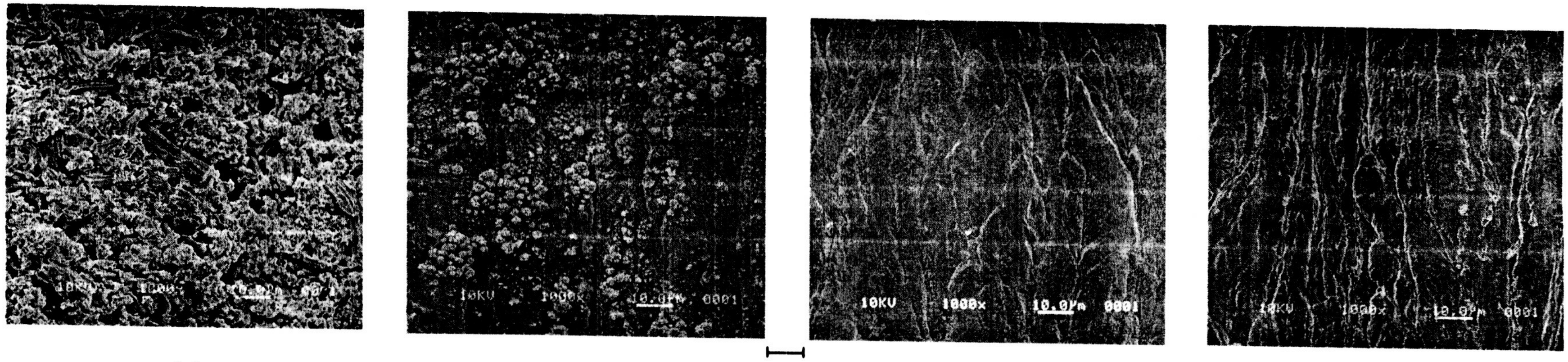

(a) (b) 10 µm (c) (d)

Figure 4. Copper test section internal surface micrographs (1000X magnification), 6 inches into the heated portion of the tube. (a) JP-8 fuel, sulfur content 400 ppm, 2 minute duration; (b) RP-1 fuel, sulfur content 23 ppm, 20 minute duration; (c) JP-7 fuel, sulfur content 10 ppm, 20 minute duration; (d) JP-10, sulfur content not analyzed (expected < 5 ppm), 20 minute duration.

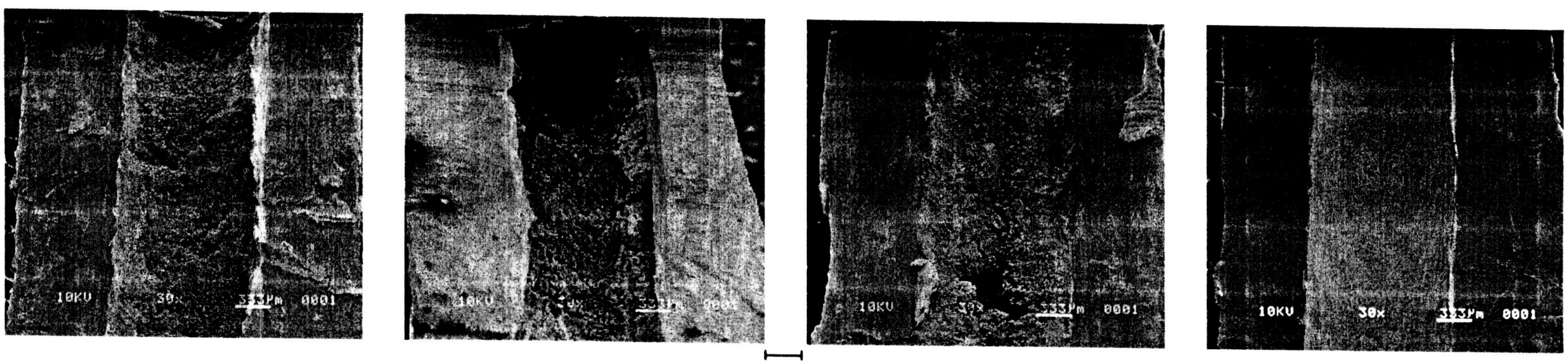

(a) (b) 333 µm (c) (d)

Figure 5. Copper test section internal surface micrographs (30X magnification) at various distances into the heated portion of the tube; JP-8 fuel, sulfur content 400 ppm, 2 minute test duration. (a) 1.5 inches; (b) 4 inches; (c) 6 inches; (d) tube outlet down stream of heated section.

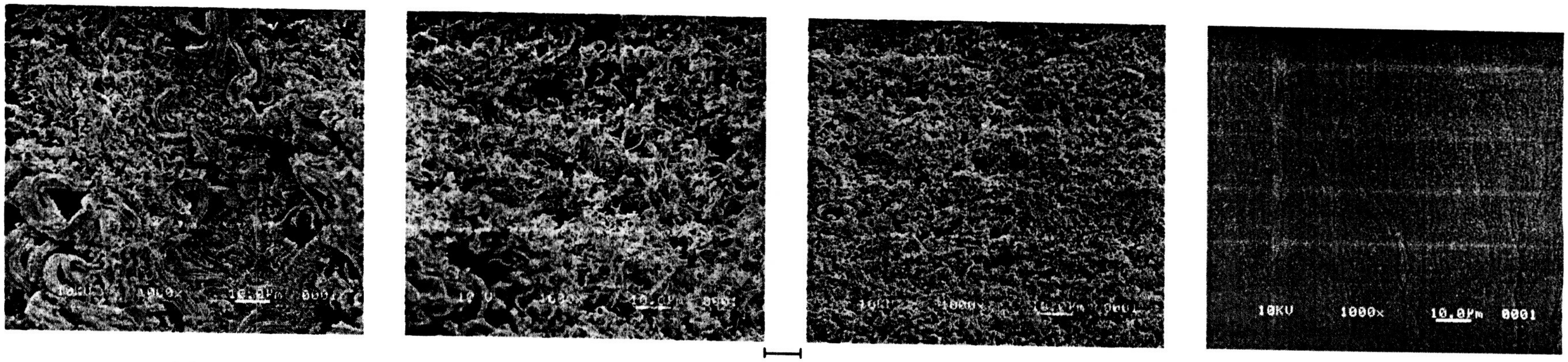

(a) (b) 10 µm (c) (d)

Figure 6. Copper test section internal surface micrographs (1000X magnification) at various distances into the heated portion of the tube; JP-8 fuel, sulfur content 400 ppm, 2 minute test duration. (a) 1.5 inches; (b) 4 inches; (c) 6 inches; (d) tube outlet down stream of heated section.

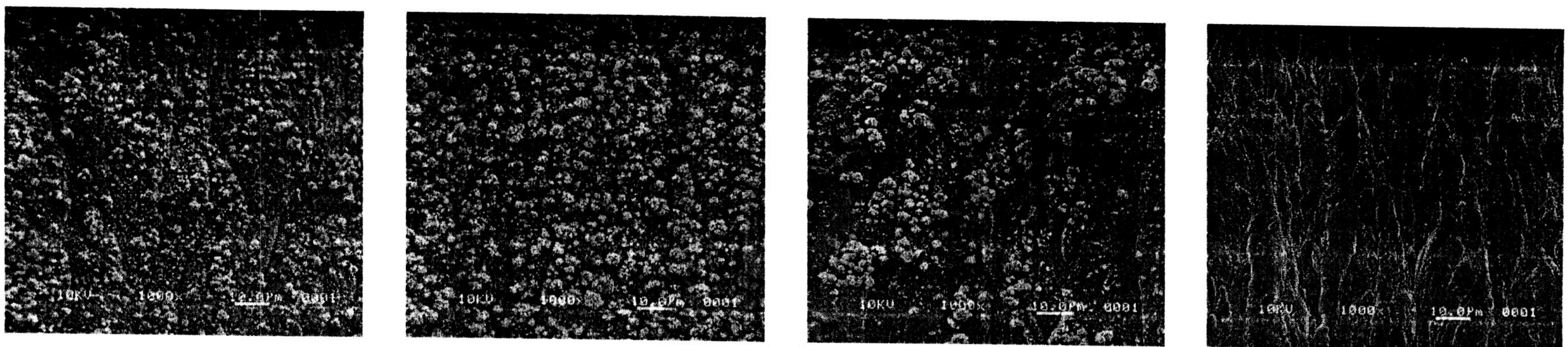

(a) (b) 10 µm (c) (d)

Figure 7. Copper test section internal surface micrographs (1000X magnification) at various distances into the heated portion of the tube; RP-1 fuel, sulfur content 23 ppm, 20 minute test duration. (a) 1.5 inches; (b) 4 inches; (c) 6 inches; (d) tube outlet down stream of heated section

The deposits formed are thin enough that the as delivered roughness of the tube wall is still visible. JP-10, a synthetic fuel, should have extremely low levels of sulfur, and formed only a thin deposit on the tube wall as well.

The deposition process is also typically dependent on the residence time that the fuel is exposed to the heated environment. Thus, it is of interest to examine any changes in the structure of the corrosion/deposition products from the inlet to the exit of the test section. Figures 5 and 6 are micrographs at 30x and 1000x from various locations along the test section from the test with JP-8. Although, it is clear that the amount of deposits increased progressing downstream in the test section, even near the entrance of the heated section the amount of material formed is significant. From the closer examination presented in figure 6, the structure of the material is dendritic all along the test section, though it appears to be more densely packed toward the exit.

A final notable observation can be made from the images taken from just downstream of the heated portion of the test section. Only a thin deposit is present and none of the dendritic structure is observed. Since even in this area the bulk temperature of the fuel is 500 °F, the formation of the dendrites appears to be driven by the higher wall temperatures in the heated test section. A similar series of micrographs (1000x only) for an RP-1 test section is presented in figure 7. In this case the dominant material formed on the walls is nodular in shape, with a thin layer of darker deposit between the nodules. Although there is a moderate change in the amount and appearance of the nodules progressing downstream, it would be difficult to draw conclusions based on these differences. As with the JP-8 test section, the micrograph from the portion of the tube just downstream of heating shows only a thin layer of darker deposit.

A representative micrograph from a SS 304 test section tested with JP-8 is included in figure 8 to illustrate the test section material effects. Only a thin darker deposit was present on the SS 304 test section without dendritic or nodular structures. The loose particles present on the surface are believed to be contamination due to an earlier sectioning technique, which used an abrasive cut-off wheel.

Qualitative observations based on the elemental compositional analyses from the EDS technique are presented in figures 9-11. One of the limitations of the EDS technique is that the focal point of the probe is larger than many of the structures of interest in the micrographs. Analyses that focused on the dendrites and nodules of figures 4(a) and 4(b) indicated that the nodules and dendrites had higher concentrations of sulfur and copper, where as the darker deposits between had higher carbon concentrations. This supports the conclusion of reference 4 that the dendritic structures contain large amounts of copper sulfides. The results of broader focal point EDS analyses were more consistent and are presented graphically. Figure 9 shows the results of the EDS analysis for each of the JP-8 test section images in figure 6. The composition appears to be relatively constant progressing down the test section. Copper and sulfur are the main components with carbon and oxygen present in lesser amounts. Figure 10 presents similar

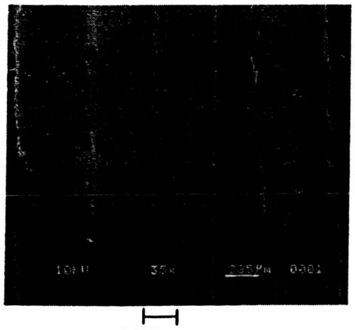

285 μm

Figure 8. Interior surface of SS 304 tube (magnification 35x) tested with JP-8 for 20 minutes; 75 ft/s, 1000 °F.

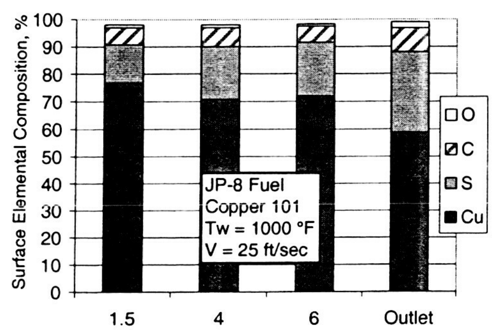

Figure 9. Tube inner wall surface elemental composition with JP-8 as a function of location in the test section.

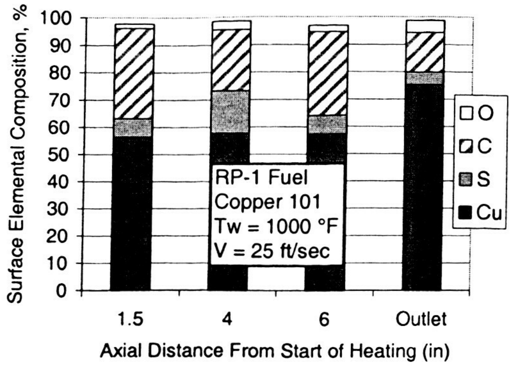

Figure 10. Tube inner wall surface elemental composition after test with RP-1 as a function of location in the test section; 20 minute duration.

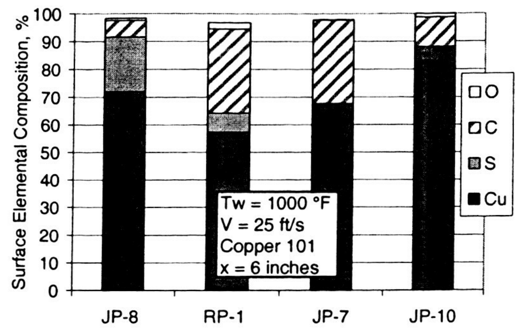

Figure 11. Tube inner wall surface elemental composition after test after 20 minutes test duration (2 minute duration for JP-8).

results for the RP-1 images in figure 7. In this case, it appears that the relative amount of carbon present is greater, and the amount of sulfur on the surface is less than the JP-8 test. This result is additional support that the dendrites that dominate the JP-8 corrosion/deposition material are due to the higher sulfur concentration. This point is made more clearly in figure 11, which presents results for each of the four fuels (images in figure 4) side-by-side for comparison. Even qualitatively, the results suggest that the sulfur content of the fuel is key to the corrosion/deposition process with copper tube materials at these conditions.

Quantitative data on the amount of carbon present on the tube surface was presented in figure 1, and indicated that significantly more carbon was deposited in the JP-8 tests than in tests with the other fuels. Based on the micrographs in figure 6, it is likely that the dendritic structure due to sulfur corrosion of the copper surface contributes to increased carbon deposition in two ways. First the dendrites serve to greatly increase the surface area where deposits can collect. Second, the dendrites form cavities where fuel can be trapped near the hot wall under stagnant or low velocity conditions and form additional solids.

SUMMARY AND CONCLUDING REMARKS

A series of electrically heated tube experiments were conducted with five readily available hydrocarbon military fuels to compare their relative thermal stability and compatibility with Stainless Steel 304 and Copper 101 materials. A previous report presented that significant carbon deposits were observed with JP-8 and JP-8+100 in Copper 101 test sections and were believed to be the result of higher sulfur content in those fuels. In this report, qualitative observations based on SEM images and EDS surface elemental composition analysis of portions of those same test sections were presented to lend insight into the mechanism of corrosion and deposition in the experiments. The images and composition analysis, although qualitative, support the proposal that the fuel-bound sulfur reacts with the copper wall material to form copper sulfides. Depending on the amount of fuel-bound sulfur present, these copper sulfide structures can be dendritic and extensive, forming a significant flow blockage.

It has been proposed that for the higher sulfur fuels, JP-8 and JP-8+100, the dendrites formed result in additional carbon deposition both through the additional surface area for collection of deposits and by creating cavities where fuel is held near the hot walls at near stagnant conditions where additional deposits form.

Finally, it is recommended that more quantitative and spatially precise (than EDS) analytical techniques be utilized to conclusively support this proposed mechanism of corrosion and deposit formation.

ACKNOWLEDGMENTS

The authors wish to acknowledge the support of Dr. Tim Edwards, Air Force Research Laboratory at Wright Patterson AFB, in providing fuels for the tests, carbon deposition measurements, and fuel sulfur analysis.

The authors are also indebted to Mary Ann Dembowski and Drago Androjna of the NASA Glenn Research Center for their efforts to obtain the high-quality SEM images and EDS analysis results presented in this report.

REFERENCES

1. Katta, V.R., Jones, E.G., and Roquemore, W.M., " Modeling of Deposition Process in Liquid Fuels," Combust. Sci. and Tech, Vol. 139, pp.75-111, 1998.

2. Volkmann, J.C., " Development of Diazidoalkane Fuel Additives for LOX/RP-1 Booster Engines," AIAA 92-3130, 1992.

3. Linne, D.L., and Munsch, W.M., "Comparison of Coking and Heat Transfer Characteristics of Three Hydrocarbon Fuels in Heated Tubes," 32nd JANNAF Combustion Meeting, CPIA Publication 631, Vol. II, pp. 95-101, October 1995.

4. Stiegemeier, B., Meyer, M. L., and Taghavi, R., "Thermal Stability and Heat Transfer Characteristics of Five Hydrocarbon Fuels: JP-7, JP-8, JP-8+100, JP-10, and RP-1," AIAA-2002-3873, 2002.

5. Schirmer, R.M., "Morphology of Deposits in Aircraft and Engine Fuel Systems," SAE Paper 700258, Society of Automotive Engineers, 1970.

6. Giovanetti, A.J., Spadaccini, L.J., and Szetela, E.J., "Deposit Formation and Heat Transfer in Hydrocarbon Rocket Fuels," NASA-CR-168277, October 1983.

7. Roback, R., Spadaccini, L.J., and Szetela, E.J., "Deposit Formation in Hydrocarbon Rocket Fuels," NASA-CR-165405, August 1981.

8. Homer, D.G., and Rosenberg, S.D., "Hydrocarbon Fuel/Combustion-Chamber-Liner Materials Compatibility," NASA CR-187104, April 1991.